Rev. Ivoir. Sci. Technol., 34 (2019) 25 - 43 25
ISSN 1813-3290, http://www.revist.ci

FRACTURE MECHANICS IN A THREE-DIMENSIONAL ELASTIC HALF-SPACE UNDER THE RECTILINEAR CONTACT PRESSURE OF A CYLINDER

P. N. B. ANONGBA

U.F.R. Sciences des Structures de la Matière et de Technologie, Université F.H.B. de Cocody, 22 BP 582 Abidjan 22, Côte d'Ivoire

* Correspondance, e-mail : *anongba@gmail.com*

ABSTRACT

This study considers a three-dimensional brittle elastic half-space on the flat Ox_1x_3- plane boundary of which an infinitely long cylinder lies along the Ox_3- contact line. Under the load P (per unit length) exerted by the cylinder along the x_2- direction, fracture propagates over large distance. The expected crack is planar with a straight front parallel to x_3, inclined with respect to x_1x_3 by an angle θ. It is expected that this angle compares well with the Hertzian conoidal crack angle produced by a spherical indenter at large distance from the indenter. The analysis of the fractured medium involves the applied stress fields; in addition to the stresses due to the cylinder by itself, the induced normal stresses originating from the Poisson's effect are considered. In this way, the x_2- component of the applied force is zero everywhere on the free surface except along the contact line. To express the stresses induced by the crack, the latter is represented by a continuous distribution of two straight edge dislocation families, parallel to x_3, with Burgers vectors along x_1 and x_2. The stress fields due to these dislocations, as well as those of a straight screw dislocation parallel to x_3, have been determined by a method involving Galerkin vectors; these results are in complete agreement with those obtained in previous works using different methods. The distribution functions of the crack dislocations under load at equilibrium satisfy a system of two integral equations with Cauchy-type singular kernels. Approximative solutions are proposed, developed in series involving the Chebyshev polynomials of first kind, the coefficients of which are evaluated numerically. Expressions of the relative displacement of the faces of the crack, crack-tip stresses and crack extension force G per unit length of the crack front are given. G displays a maximum at an angle θ that is confronted to experiment. $\partial G / \partial \theta = 0$, the condition that determines the crack angle, is seen to depend on Poisson's ratio only. The expression for G is useful in spherical indentation fracture too.

Keywords : *fracture mechanics, linear elasticity, dislocations, Galerkin vector, singular integral equations, Poisson effect.*

RÉSUMÉ

Mécanique de la rupture dans un demi-espace élastique à trois dimensions sous la pression de contact rectiligne d'un cylindre

Cette étude considère un demi-espace élastique fragile à trois dimensions avec comme surface le plan Ox_1x_3, sur lequel un cylindre infiniment long est couché, le long de la ligne de contact Ox_3. Sous la charge P (par unité de longueur) exercée par le cylindre dans la direction x_2, la rupture se propage sur une grande distance. La fissure attendue est plane avec un front droit parallèle à x_3, inclinée par rapport à x_1x_3 d'un angle θ. On s'attend à ce que cet angle soit bien comparable à l'angle de fissure conoïdal hertzien produit par un indenteur sphérique, à grande distance de l'indenteur. L'analyse du milieu fracturé implique les champs de contraintes appliquées ; en plus des contraintes dues au cylindre lui-même, les contraintes normales induites provenant de l'effet de Poisson sont également prises en compte. Pour exprimer les contraintes induites par la fissure, celle-ci est représentée par une distribution continue de deux familles de dislocations coins droites, parallèles à x_3, avec des vecteurs de Burgers suivant x_1 et x_2. Les champs de contraintes dus à ces dislocations, ainsi que ceux d'une dislocation vis droite parallèle à x_3, ont été déterminés par une méthode impliquant des vecteurs de Galerkin; ces résultats sont en parfait accord avec ceux obtenus lors de travaux antérieurs utilisant différentes méthodes. Les fonctions de distribution des dislocations de fissure, sous charge à l'équilibre, satisfont un système de deux équations intégrales singulières de type Cauchy. Des expressions des fonctions de distribution des dislocations de fissure, du déplacement relatif des lèvres de la fissure, de contraintes en tête de fissure et de la force d'extension G de la fissure (par unité de longueur du front de fissure) sont données. G affiche un maximum à un angle θ qui est confronté à l'expérience. $\partial G / \partial \theta = 0$, la condition qui détermine l'angle d'inclinaison de la fissure, dépend uniquement du module de Poisson. L'expression de G est également utile dans les fractures à indentation sphérique.

Mots-clés : *mécanique de la rupture, dislocation, vecteur de Galerkin, équation intégrale singulière, effet Poisson*.

I - INTRODUCTION

In the present study, by "Fracture Mechanics", it is meant a crack analysis that incorporates the relative displacement of the faces of the crack, crack-tip stresses, crack extension force G per unit edge length of the crack and fracture spatial extension using the Griffith concept $G = 2\gamma$ (γ is the surface energy). We shall look for crack configurations that maximize G. This is in these configurations that the condition $G = 2\gamma$ is applied and confronted with experiments. The considered crack system is depicted in ***Figure 1***. This is a three-dimensional infinitely extended brittle elastic half-space on the flat surface of which a contact pressure is exerted by a cylinder. We assume that fracture propagation occurs over large distance in the medium and focus our attention on the crack-tip *B* that is moving away from the cylinder. Hence, the nucleation of the crack and what happens about the cylinder is out of scope. Rather we seek the crack natural configuration under load through its length *l* and inclination angle θ from the medium flat boundary.

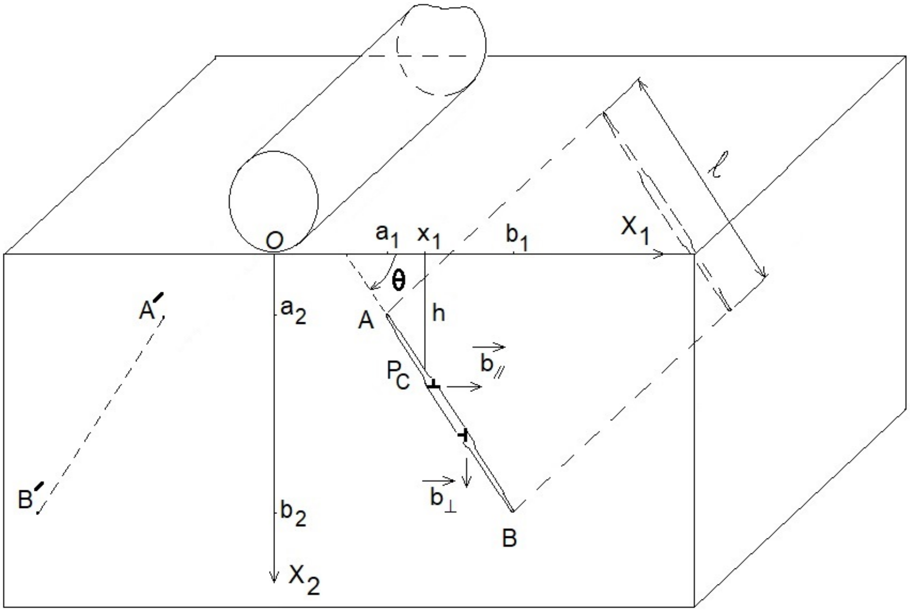

Figure 1 : *Brittle elastic half-space under load by a cylinder (P is the load per unit length of the cylinder) posed along the* x_3*- direction on its flat boundary surface; a planar crack of finite extension l is present, located between positions A and B in the* Ox_1x_2 *- plane and inclined by angle* θ *from the planar boundary. The crack front is straight, parallel to the cylinder axis. Our modelling assumes the half-space to be infinitely extended and the cylinder and crack to run indefinitely along the* x_3*- direction*

More specifically ***(Figure 1)***, with respect to a Cartesian axis system x_i, the cylinder of infinite length (load *P* per unit length) is posed on the Ox_3- axis. The crack is assumed planar with a straight front parallel to x_3 and located (schematically) between spatial positions *A* (a_1, a_2 ,0) (may be coincident with *O*) and *B* (b_1, b_2 ,0) in the Ox_1x_2- plane; it is inclined by angle θ around the Ax_3-axis with respect to x_1x_3. The crack of finite length *l* extends along x_1 from

$x_1 = a_1$ to $b_1 = a_1 + l \cos \theta$, x_2 from $x_2 = a_2$ to $b_2 = a_2 + l \sin \theta$ and runs indefinitely in the x_3- direction. The relevance of this modelling may be understood as follows. A slab of cylinder with thickness $dx_3^{'}$ at spatial position O' $(0,0,x_3^{'})$ exerts elastic fields (displacement and stress) proportional to those of a point load at O' (proportionality coefficient $dx_3^{'}$). Physically, this corresponds to the action of a spherical indenter to which is associated a conoidal fracture surface for sufficiently large load (Roesler (1956) [1] as quoted by Frank and Lawn (1967) [2]; see also [3]). The coalescence of conoidal cracks from different slabs of cylinder along Ox_3 would produce planar fracture surface envelops parallel to x_3 at large crack lengths. Therefore, we expect our modelling to provide the experimentally observed fracture surface inclination angle θ and crack length l as a function of critical load P by both a spherical indenter and cylinder. A symmetrical crack with respect to Ox_2x_3 is expected to develop between A' and B'. This is considered by replacing P by $P/2$ in the various expressions obtained in the analysis with only one crack; this corresponds to increasing the critical load at fracture in $G = 2\gamma$ by a factor 2. As in our previous crack analyses (see [4 - 7], among others), the crack under load is represented by a continuous distribution of dislocations with infinitesimal Burgers vectors. The stress induced by the crack is equivalent to that produced by the dislocations.

Two straight edge dislocation families J (J= // and $\perp$) parallel to x_3 with Burgers vectors $\vec{b}_{//} = (b,0,0)$ and $\vec{b}_{\perp} = (0,b,0)$ parallel and perpendicular to the solid flat surface are considered. To a crack dislocation J located at x_1 is associated an elevation h from Ox_1x_3 ***(Figure 1)*** with distribution function D_J such that $D_J(x_1^{'})dx_1^{'}$ represent the number of crack dislocations J in small x_1-interval $dx_1^{'}$ about $x_1^{'}$. It is required to find the equilibrium dislocation distributions under the combined actions of the cylinder and the crack dislocations. The applied stress tensor $(\sigma)^A$ will include the stress $(\sigma)^a$ due to the cylinder itself and the induced normal stresses due to the Poisson effect, namely that, to a normal stress σ_{ii}^a acting in the x_i- direction also correspond normal stresses ($-\nu\sigma_{ii}^a$) in the two other associated x_j - directions. It is important to mention that considering the induced normal stresses due to Poisson effect is in fact necessary for the x_2- component of the applied force exerted on a boundary surface element ds, at any spatial position P_S of the three-dimensional elastic half-space flat boundary, to be zero except on Ox_3 (Section 3). Stress fields due to straight edges in half- space are available [8, 9]. We provide below dislocation J elastic fields from a different method involving Galerkin vectors with biharmonic functions in Fourier forms; a similar procedure has been used to investigate the elastic fields of interfacial dislocations (straight and sinusoidal) [10 - 12]. In what follows, the methodologies for determining $(\sigma)^A$, dislocation stress fields $(\sigma)^{(J)}$ and crack analysis are given in Section 2. In Section 3 are listed the various applied and dislocation stress expressions, crack dislocation distributions, crack-tip stresses and crack extension force. Numerical analysis and discussion form Section 4. Section 5 is devoted to the conclusion.

II - METHODOLOGY

II-1. Applied elastic fields

The displacement corresponding to a pressure at a point on a plane boundary may be taken from Love [13]; we assume a slab of cylinder of thickness $dx_3^{'}$, located at $O'(0,0,x_3^{'})$ and acting in the x_2 - direction, to produce a displacement corresponding to that of a pressure point multiplied by $dx_3^{'}$. This gives by superposition the displacement $\vec{u}^{\,a}$ produced by the cylinder, at arbitrary position (x_1, x_2, x_3), in the form

$$u_1^a = \frac{Px_1x_2}{4\pi\mu}\int_{-\infty}^{\infty}\frac{dx_3^{'}}{r'^3} - \frac{Px_1}{4\pi(\lambda+\mu)}\int_{-\infty}^{\infty}\frac{dx_3^{'}}{r'(x_2+r')},$$
$$u_2^a = \frac{Px_2^2}{4\pi\mu}\int_{-\infty}^{\infty}\frac{dx_3^{'}}{r'^3} + \frac{P(\lambda+2\mu)}{4\pi\mu(\lambda+\mu)}\int_{-\infty}^{\infty}\frac{dx_3^{'}}{r'},$$
$$u_3^a = 0; \tag{1}$$

$r'^2 = x_1^2 + x_2^2 + (x_3 - x_3^{'})^2$ and λ and μ are Lamé's constants. The associated stress fields $(\sigma)^a$ are obtained from the displacement $\vec{u}^{\,a}$ by partial differentiation with respect to coordinates x_i. As introduced in Section 1, induced normal stresses originating from Poisson effect are considered; hence, the applied stress field $(\sigma)^A$ has the form

$$(\sigma)^A = \begin{pmatrix} \sigma_{11}^a - \nu(\sigma_{22}^a + \sigma_{33}^a) & \sigma_{12}^a & 0 \\ \sigma_{12}^a & \sigma_{22}^a - \nu(\sigma_{11}^a + \sigma_{33}^a) & 0 \\ 0 & 0 & \sigma_{33}^a - \nu(\sigma_{11}^a + \sigma_{22}^a) \end{pmatrix}. \tag{2}$$

σ_{ij}^a *are listed in Section 3. It is revealed that* $\sigma_{33}^A = 0$.

II-2. Elastic fields of straight dislocations in a half-space

We consider here a three-dimensional half-space (infinitely extended elastic solid) with shear modulus μ and Poisson's ratio ν. The solid occupies the region $x_2 > 0$ and its flat surface is Ox_1x_3; it contains a straight dislocation parallel to x_3 and displaced by $x_2 = h$ from the origin ***(Figure 2)***. The dislocations concerned

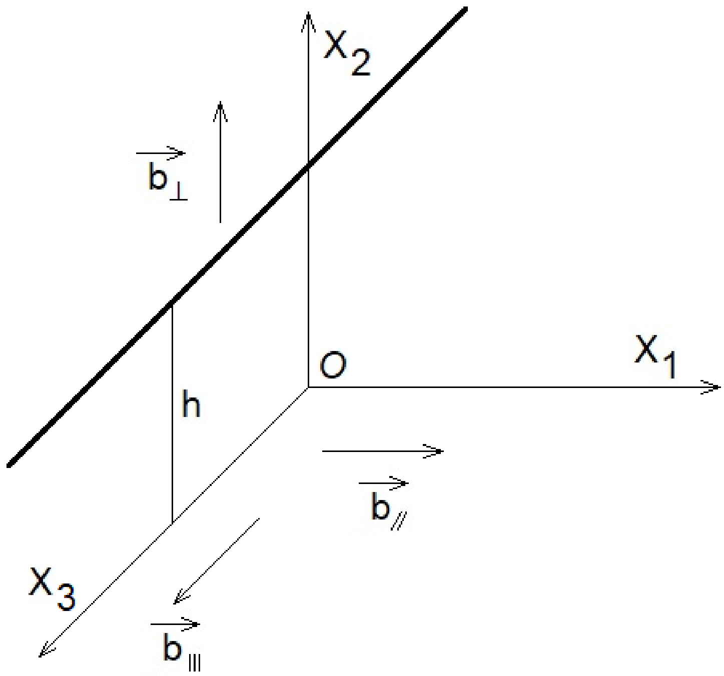

Figure 2 : *Elastic half-space $x_2 > 0$ containing an infinitely long straight dislocation J parallel to x_3 and displaced by $x_2 = h$ from the origin with Burgers vector $\vec{b}_J$ directed along x_1 (J= //), x_2 (J =⊥) or x_3 (J = III)*

are edges with Burgers vectors $\vec{b}_{//} = (b, 0, 0)$ parallel to x_1 and $\vec{b}_{\perp} = (0, b, 0)$ parallel to x_2 ***(Figure 2)***. We present below a methodology for determining their elastic fields that is equally valid for a screw dislocation with Burgers vector $\vec{b}_{III} = (0, 0, b)$. Let $\vec{u}^{(J)}$ and $(\sigma)^{(J)}$ be the displacement and stress fields in the medium due to the dislocation J (J= //, ⊥ and *III*). Very generally, the following description is expected to apply:

- The surface Ox_1x_3 is free from traction; at P_s (x_1, 0, x_3), this gives

$$\sigma_{12}^{(J)} = 0 \, , \; \sigma_{22}^{(J)} = 0 \text{ and } \sigma_{23}^{(J)} = 0 \, . \qquad (3)$$

- Far from the dislocation and free surface, the elastic fields correspond to those ($\vec{u}^{(J)\infty}$, $(\sigma)^{(J)\infty}$) of a straight dislocation displaced by $x_2 = h$ from the origin with Burgers vector $\vec{b}_J$ in the whole three-dimensional space; hence

$$\begin{aligned} &\vec{u}^{(J)} \to \vec{u}^{(J)\infty} \\ &(\sigma)^{(J)} \to (\sigma)^{(J)\infty} \end{aligned} \tag{4}$$

when one moves far away in the x_2- direction ($|x_2 - h| \to \infty$).

- The elastic fields may be expressed in the form

$$\begin{aligned} &\vec{u}^{(J)} = \vec{u}^{(J)\infty} - \vec{u}^{(J)W} \\ &(\sigma)^{(J)} = (\sigma)^{(J)\infty} - (\sigma)^{(J)W} \end{aligned} \tag{5}$$

where $\vec{u}^{(J)W}$ and $(\sigma)^{(J)W}$ satisfy the equations of equilibrium and possess the following properties.

$$\begin{aligned} &\vec{u}^{(J)\infty}(P_S) = \vec{u}^{(J)W}(P_S) \\ &(\sigma)^{(J)\infty}(P_S) = (\sigma)^{(J)W}(P_S)\,; \end{aligned} \tag{6}$$

this ensures the traction-free boundary condition (3).

- $\vec{u}^{(J)W}$ and $(\sigma)^{(J)W}$ cancel far from free surface and dislocation; this means that

$$\begin{aligned} &\vec{u}^{(J)W} \to 0 \\ &(\sigma)^{(J)W} \to 0 \end{aligned} \tag{7}$$

when $|x_2 - h| \to \infty$; this ensures the veracity of (4) above.

The elastic fields $\vec{u}^{(J)}$ and $(\sigma)^{(J)}$ thus obtained are valuable representations to ***Figure 2***. The associated $\vec{u}^{(J)W}$ and $(\sigma)^{(J)W}$ are investigated with the help of Galerkin vectors in a similar way as in our previous works [10 - 12]. We take Galerkin vectors $\vec{V}^{(J)}$ with only one non-zero , x_1- component $V_1^{(//)}$ for $J = //$, x_2- component $V_2^{(\perp)}$ for $J = \perp$, and x_3- component $V_3^{(III)}$ for $J = III$, with same form

$$V_j^{(J)}(\vec{x}) = \bar{\alpha}^{(J)}(\vec{k})e^{i\vec{k}.\vec{x}} + \bar{\beta}^{(J)}(\vec{k})x_2 e^{i\vec{k}.\vec{x}}, \tag{8}$$

$j = 1$ to 3 for $J = //, \perp, III$ respectively, under the condition $\vec{k}^2 = k_1^2 + k_2^2 + k_3^2 = 0$ that ensures the biharmonicity of $V_j^{(J)}$. For $V_j^{(J)}$ to cancel far from the dislocation and free surface, we take $k_2 = i\sqrt{k_1^2 + k_3^2}$. The elastic fields under consideration are x_3- independent; hence k_3 is set equal to zero. This leads to

$$k_2 = i|k_1|. \tag{9}$$

The elastic fields corresponding to $V_j^{(J)}$ (8) may be first calculated (see [10], for example); then more general forms $\vec{u}^{(J)W}$ and $(\sigma)^{(J)W}$ are constructed from the previous ones by superposition over k_1. To calculate $\bar{\alpha}^{(J)}$ and $\bar{\beta}^{(J)}$ (8), we use (6) for the stress and restrict ourselves to stress components involved in the traction-free boundary condition (3) only. $(\sigma)^{(J)\infty}$ is taken from [4] and written in Fourier forms at P_S. We obtain

$$\begin{aligned}
\bar{\alpha}^{(//)} &= \frac{iC_1}{2k_1^3}\left(-2 + 2\nu + (5-4\nu)h|k_1|\right)e^{-h|k_1|}, \\
\bar{\beta}^{(//)} &= \frac{iC_1}{2k_1^2}\left(-1 + 2h|k_1|\right)\mathrm{sgn}(k_1)e^{-h|k_1|}; \\
\bar{\alpha}^{(\perp)} &= \frac{iC_1}{2k_1^3}\left(-2\nu + (1-4\nu)h|k_1|\right)e^{-h|k_1|}, \\
\bar{\beta}^{(\perp)} &= -\frac{iC_1}{2k_1^2}\left(1 + 2h|k_1|\right)\mathrm{sgn}(k_1)e^{-h|k_1|}; \\
\bar{\alpha}^{(III)} &= 0, \\
\bar{\beta}^{(III)} &= -\frac{iD_1}{4(1-\nu)}\frac{\mathrm{sgn}(k_1)}{k_1^2}e^{-h|k_1|};
\end{aligned} \tag{10}$$

$C_1 = \mu b / 2\pi(1-\nu)$, $D_1 = \mu b / 2\pi$. Again with (10), $\vec{u}^{(J)W}$ and $(\sigma)^{(J)W}$ are known; the associated dislocation J elastic fields are given by (5).

II-3. Crack analysis

We consider one crack in the half-space, located between A and B in the Ox_1x_2-plane ***(Figure 1)*** as described in Section 1. The crack system is completely defined when the dislocation distributions D_J (J= // and $\perp$) are known. For this purpose, we ask the crack faces to be free from traction; this gives

$$\begin{cases} \bar{\sigma}_{12} - \partial h / \partial x_1 \bar{\sigma}_{11} = 0 \\ \bar{\sigma}_{22} - \partial h / \partial x_1 \bar{\sigma}_{12} = 0 \end{cases}. \tag{11}$$

$(\bar{\sigma})$ is the stress at any position $P(x_1, x_2, x_3)$ in the medium and is linked to D_J. In (11), we are concerned with the point $P_C(x_1, x_2 = h(x_1), x_3)$ of the crack faces only. We write

$$(\bar{\sigma}) = (\sigma)^A + (\bar{\sigma})^{(//)} + (\bar{\sigma})^{(\perp)}; \tag{12}$$

$(\sigma)^A$ (2) is the applied stress $(\sigma)^a$ due to the cylinder including induced normal stresses originating from the Poisson effect; $\bar{\sigma}_{ij}^{(J)}$ has the form

$$\bar{\sigma}_{ij}^{(J)}(P) = \int_{a_1}^{b_1} \sigma_{ij}^{(J)}(x_1 - x_1^{'}, x_2, x_3) D_J(x_1^{'}) dx_1^{'} \quad (J = // \text{ and } \perp). \tag{13}$$

$\sigma_{ij}^{(J)}$ is the stress produced by a dislocation J located at an elevation $h(x_1^{'})$ from the half-space boundary. (11) provides two integral equations with Cauchy-type singular kernels that determine the D_J. When these have been found, the relative displacement of the faces of the crack, crack-tip stresses and crack extension force are obtained by integrations (Section 3). In what follows, our calculation results are displayed in the order defined in the methodology Section 2.

III - RESULTS

III-1. Applied elastic fields

The displacement $\vec{u}^a$ ($r^2 = x_1^2 + x_2^2$, $r \neq 0$) obtained from (1) is :

$$u_1^a = \frac{P}{2\pi\mu}\left(2(1-2\nu)\frac{x_1 \ln r}{x_2} + \frac{x_1 x_2}{r^2} - 2(1-2\nu)\tan^{-1}\frac{x_1}{x_2 + r}\right),$$

$$u_2^a = \frac{P}{2\pi\mu}\left(-2(1-\nu)\ln r + \frac{x_2^2}{r^2}\right),$$

$$u_3^a = 0. \tag{14}$$

Constants with infinite values are omitted. We use (14) for $x_2 \neq 0$. Arguments in the logarithm are dimensionless. These conditions also apply for the corresponding stress $(\sigma)^a$ that follows:

$$(\sigma)^a = \begin{pmatrix} \sigma_{11}^a & \sigma_{12}^a & 0 \\ \sigma_{12}^a & \sigma_{22}^a & 0 \\ 0 & 0 & \sigma_{33}^a \end{pmatrix};$$

$$\sigma_{11}^a = \frac{2P}{\pi x_2}\left((1-\nu)\ln r + \frac{(1-\nu)x_1^2}{r^2} - \frac{x_1^2 x_2^2}{r^4} \right),$$

$$\sigma_{22}^a = \frac{2P}{\pi x_2}\left(\nu \ln r + \frac{\nu x_1^2}{r^2} - \frac{x_2^4}{r^4} \right),$$

$$\sigma_{33}^a = \frac{2\nu P}{\pi x_2}\left(\ln r + \frac{x_1^2 - x_2^2}{r^2} \right),$$

$$\sigma_{12}^a = -\frac{P x_1}{\pi x_2^2}\left((1-2\nu)\ln r - \frac{(1-2\nu)x_2^2}{r^2} + \frac{2x_2^4}{r^4} \right). \tag{15}$$

The applied stress field $(\sigma)^A$ (2) becomes

$$(\sigma)^A = \begin{pmatrix} \sigma_{11}^A & \sigma_{12}^a & 0 \\ \sigma_{12}^a & \sigma_{22}^A & 0 \\ 0 & 0 & 0 \end{pmatrix};$$

$$\sigma_{11}^A = \frac{2(1+\nu)P}{\pi x_2}\left((1-2\nu)\ln r + \frac{(1-2\nu)x_1^2 - (1-\nu)x_2^2}{r^2} + \frac{x_2^4}{r^4} \right),$$

$$\sigma_{22}^A = \frac{2P x_2}{\pi r^2}\left(\nu^2 + \frac{\nu x_1^2 - x_2^2}{r^2} \right). \tag{16}$$

The traction $d\vec{F}_H$ at an arbitrary point on any surface element *ds* parallel to x_1x_3 is given by

$$\frac{d\vec{F}_H}{ds} = \begin{pmatrix} \sigma_{12}^a \\ \sigma_{22}^A \\ 0 \end{pmatrix}. \tag{17}$$

At P_s (x_1, 0, x_3), the component σ_{22}^{A} perpendicular to the boundary plane Ox_1x_3 vanishes when $x_2 \rightarrow 0$, except at r= 0, as expected. $\sigma_{33}^{A} = 0$ is equally wanted. Hence, $(\sigma)^{A}$ (16) behaves adequately.

III-2. Dislocation stress fields

Galerkin vectors $\vec{V}^{(J)}$ (8, 10), $J = //, \perp$ and III, have been used to estimate the dislocation elastic fields. We display below the stresses only because there are involved in the crack analysis.

$$\sigma_{ii}^{(\perp)} = C_1 x_1 \left(\frac{\delta_{i1} + \delta_{i2} + 2\nu\delta_{i3}}{r_{-h}^2} + \frac{2(x_2 - h)^2(\delta_{i2} - \delta_{i1})}{r_{-h}^4} - \frac{\delta_{i1} + \delta_{i2} + 2\nu\delta_{i3}}{r_{+h}^2} \right.$$
$$- \frac{2(x_2 + h)\left(\delta_{i2}(x_2 + h) - \delta_{i1}(x_2 - 3h) + \delta_{i3} 4\nu h\right)}{r_{+h}^4}$$
$$\left. + \frac{4hx_2\left(3(x_2 + h)^2 - x_1^2\right)(\delta_{i1} - \delta_{i2})}{r_{+h}^6} \right),$$

$$\sigma_{12}^{(\perp)} = C_1 \left(\frac{(x_2 - h)\left(x_1^2 - (x_2 - h)^2\right)}{r_{-h}^4} + \frac{(x_2 - h)\left((x_2 + h)^2 - x_1^2\right)}{r_{+h}^4} \right.$$
$$\left. + \frac{4hx_2(x_2 + h)\left((x_2 + h)^2 - 3x_1^2\right)}{r_{+h}^6} \right),$$

$$\sigma_{j3}^{(\perp)} = 0\,; \tag{18}$$

$$\sigma_{ii}^{(//)} = C_1 \left(- \frac{(x_2 - h)\left(\delta_{i1} - \delta_{i2} + 2\nu\delta_{i3}\right)}{r_{-h}^2} - \frac{2(x_2 - h)\left(\delta_{i1} x_1^2 + \delta_{i2}(x_2 - h)^2\right)}{r_{-h}^4} \right.$$
$$+ \frac{x_2(3\delta_{i1} - \delta_{i2} + 2\nu\delta_{i3}) + h(5\delta_{i1} + \delta_{i2} + 2\nu\delta_{i3})}{r_{+h}^2} + \frac{16hx_2(x_2 + h)^3(\delta_{i1} - \delta_{i2})}{r_{+h}^6}$$
$$+ \frac{\delta_{i3} 4h\nu\left(x_1^2 - (x_2 + h)^2\right)}{r_{+h}^4}$$
$$\left. + \frac{2(x_2 + h)\left((x_2 + h)\left[x_2(\delta_{i2} - \delta_{i1}) - h(3\delta_{i1} + \delta_{i2})\right] + 6hx_2(\delta_{i2} - \delta_{i1})\right)}{r_{+h}^4} \right),$$

$$\sigma_{12}^{(//)} = C_1 x_1 \left(\frac{x_1^2 - (x_2 - h)^2}{r_{-h}^4} - \frac{x_1^2 - (x_2 + h)^2}{r_{+h}^4} - \frac{4hx_2\left(3(x_2 + h)^2 - x_1^2\right)}{r_{+h}^6} \right),$$

$$\sigma_{j3}^{(II)} = 0 ; \tag{19}$$

$$\sigma_{j3}^{(III)} = D_1 \left(\frac{\delta_{j1}(h - x_2) + \delta_{j2} x_1}{r_{-h}^2} + \frac{\delta_{j1}(h + x_2) - \delta_{j2} x_1}{r_{+h}^2} \right),$$

$$\sigma_{ii}^{(III)} = 0 , \ \sigma_{12}^{(III)} = 0 . \tag{20}$$

In (18 - 20), δ_{ij} is the Kronecker delta, subscripts i and j take values (1, 2 and 3) and (1 and 2), respectively; $r_{-h}^2 = x_1^2 + (x_2 - h)^2$, $r_{+h}^2 = x_1^2 + (x_2 + h)^2$, $C_1 = \mu b / 2\pi(1-\nu)$, $D_1 = \mu b / 2\pi$. These results are in complete agreement with previous works [8, 9].

III-3. Crack dislocation distributions

With $(\sigma)^A$ (16) and $(\sigma)^{(J)}$ (18, 19), the condition (11) can be written in the form

$$\begin{cases} f_{//}^A(x_1) + D_{\perp}^C(x_1) + \int_{a_1}^{b_1} dx_1' D_{//}(x_1') C_1 \left(\frac{1}{x_1 - x_1'} + d_{//}(x_1, x_1') \right) = 0 \\ f_{\perp}^A(x_1) + D_{//}^C(x_1) + \int_{a_1}^{b_1} dx_1' D_{\perp}(x_1') C_1 \left(\frac{1}{x_1 - x_1'} + d_{\perp}(x_1, x_1') \right) = 0 \end{cases} ; \tag{21}$$

$$f_{//}^A = \sigma_{12}^A - p_0 \sigma_{11}^A , \ f_{\perp}^A = \sigma_{22}^A - p_0 \sigma_{12}^A , \ p_0 = \tan\theta ; \tag{22}$$

$$D_{\perp}^C(x_1) = \int_{a_1}^{b_1} dx_1' D_{\perp}(x_1') C_1 \left(p_0 \left[d_{//}(x_1, x_1') - d_{\perp}(x_1, x_1') \right] + d_C(x_1, x_1') \right),$$

$$D_{//}^C(x_1) = -\int_{a_1}^{b_1} dx_1' D_{//}(x_1') C_1 d_C(x_1, x_1') ; \tag{23}$$

$$d_{\perp}(x_1, x_1') = \frac{Num\ d_{\perp}}{\rho_{hh'}^6},$$

$$Num\ d_{\perp} = (x_1' - x_1)\Big((1 + 3p_0^2)(x_1 - x_1')^4 - 12hh' p_0 (x_1 - x_1')(h + h')$$
$$+ (h + h')^2 \left[(3 + p_0^2)(h + h')^2 + 12hh' \right] \Big) + 4hh' p_0 (h + h')^3 ,$$

$$d_{//}(x_1, x_1') = d_{\perp}(x_1, x_1') + \frac{(x_1 - x_1') 8h'(h + h')}{\rho_{hh'}^4},$$

$$d_C(x_1, x_1^{'}) = \frac{4hh'}{\rho_{hh'}^6}\Big((h+h')^3 - 3(x_1 - x_1^{'})^2(h+h')$$
$$-3p_0(x_1 - x_1^{'})(h+h')^2 + p_0(x_1 - x_1^{'})^3\Big); \qquad (24)$$

$x_2 = h(x_1) = p_0 x_1 + h_0$ (h_0 is constant),

$$h' = h(x_1^{'}),\ \rho_{hh'}^2 = (x_1 - x_1^{'})^2 + (h+h')^2 . \qquad (25)$$

We stress that $d_\perp$, $d_{//}$ and d_C are continuous and bounded for $p_0 \neq 0$. Following works by Erdogan and Gupta [14, 15] (see also [16, 17]), we propose to (21), the following approximate solution

$$D_J(x_1) = \frac{\overline{ba}_1 f_J^A(b_1)}{C_1} D_0(\overline{x}_1) \sum_{n=1}^{N} \alpha_n^{(J)} T_n(\overline{x}_1 / \overline{ba}_1),\ |\overline{x}_1| < \overline{ba}_1; \qquad (26)$$

$D_0 = 1/\pi\sqrt{\overline{ba}_1^{\,2} - \overline{x}_1^2}$, $\overline{x}_1 = x_1 - (a_1 + b_1)/2$, $\overline{ba}_1 = (b_1 - a_1)/2$, and $J = //$ and $\perp$. T_n are the Chebyshev polynomials of first kind, N and the coefficients $\alpha_n^{(J)}$ are obtained numerically (similarly as in [16], for example); this will be the subject of Section 4. The relative displacement of the faces of the crack in the x_1-direction $\phi_{//}$ and x_2- direction $\phi_\perp$ are given by $d\phi_J = -bD_J(x_1)dx_1$; this gives

$$\phi_J(x_1) = \frac{b\overline{ba}_1 f_J^A(b_1)}{\pi C_1} \sum_{n=1}^{N} \frac{\alpha_n^{(J)} \sin\left(n\cos^{-1}(\overline{x}_1 / \overline{ba}_1)\right)}{n},\quad |\overline{x}_1| \leq \overline{ba}_1 . \qquad (27)$$

Here the constant of integration is set equal to zero so that $\phi_J(\pm\overline{ba}_1) = 0$. Thus, it appears that D_J is unbounded at $\overline{x}_1 = \pm\overline{ba}_1$ and the ϕ_J curve is vertical at these end points. This behavior is known from the study of planar cracks [18]. We stress that (26) is intended to capture the crack-tip characteristic functions at $x_1 = b_1$ only, for sufficiently large crack length l. What happens at $x_1 = a_1$ about the cylinder ***(Figure 1)*** is out of scope; in practice, the region about the cylinder is associated with damage material and irreversible processes when fracture occurs over large distance.

III-4. Crack-tip stresses

In the crack plane and ahead of the crack-tip at spatial position $P_C(x_1 = b_1 + s, x_2 = h(x_1), x_3)$, $0 < s << b_1$, the total stress $\overline{\sigma}_{ij}(P_C)$ is identified to the following formula

$$\bar{\sigma}_{ij}(s) = \sum_{J=//\text{and}\perp} \int_{b_1-\delta b_1}^{b_1} \bar{\sigma}_{ij}^{(J)}(b_1 + s - x_1^{'}) D_J(x_1^{'}) dx_1^{'}, \quad \delta b_1 << b_1 . \tag{28}$$

This formula means that only those dislocations located about the crack front in x_1- interval $[b_1 - \delta b_1, b_1]$ will contribute significantly to the stress at $x_1 = b_1 + s$ ahead of the crack-tip as s tends to zero; any other contribution will become negligible for a sufficiently small value of s. Using (26) for D_J and integrating (28), we obtain

$$\bar{\sigma}_{12}(s) = \frac{(1-p_0^2)\sqrt{\overline{ba_1}}}{(1+p_0^2)^2\sqrt{2s}}\left(p_0 f_\perp^A(b_1)\Omega^{(\perp)} + f_{//}^A(b_1)\Omega^{(//)} \right),$$
$$\bar{\sigma}_{11}(s) = \frac{\sqrt{\overline{ba_1}}}{(1+p_0^2)^2\sqrt{2s}}\left((1-p_0^2) f_\perp^A(b_1)\Omega^{(\perp)} - p_0(3+p_0^2) f_{//}^A(b_1)\Omega^{(//)} \right),$$
$$\bar{\sigma}_{22}(s) = \frac{\sqrt{\overline{ba_1}}}{(1+p_0^2)^2\sqrt{2s}}\left((1+3p_0^2) f_\perp^A(b_1)\Omega^{(\perp)} + p_0(1-p_0^2) f_{//}^A(b_1)\Omega^{(//)} \right),$$
$$\bar{\sigma}_{33}(s) = \frac{2\nu\sqrt{\overline{ba_1}}}{(1+p_0^2)\sqrt{2s}}\left(f_\perp^A(b_1)\Omega^{(\perp)} - p_0 f_{//}^A(b_1)\Omega^{(//)} \right),$$
$$\bar{\sigma}_{j3} = 0, \quad j = 1 \text{ and } 2; \tag{29}$$

$$\Omega^{(//)} = \sum_{n=1}^{N} \alpha_n^{(//)}, \quad \Omega^{(\perp)} = \sum_{n=1}^{N} \alpha_n^{(\perp)} . \tag{30}$$

We mention that $\overline{ba_1}$ can be expressed in terms of crack length l as $\overline{ba_1} = l / \; 2\sqrt{1+p_0^2}$.

III-5. Crack extension force

Our definition of the crack extension force is taken from [18] and used extensively (see [4 - 7, 16], for example). A crack of length l is considered at equilibrium under load (use ***Figure 1*** for illustration). Then, this crack grows almost statically over a short distance from one of its ends (say $x_1 = b_1$) while the other end remains fixed. A work associated with a newly created surface element Δs is then calculated, which is the product of the elastic force (using (29)) on the element (just before the motion of the crack tip) by the relative displacement of the faces of the newly created crack through Δs

(using (27)). This energy is then divided by Δs ; the limit G taken by the ratio of that energy divided by Δs when the latter tends to zero is by definition the crack extension force per unit length of the crack front at the point P_C where Δs is located. We obtain at B (b_1, $h(b_1)$, x_3)

$$G(B) = \frac{(1-\nu)l}{\mu(1+p_0^2)}\left(\left[f_{\perp}^{A}(b_1)\Omega^{(\perp)}\right]^2 + \left[f_{//}^{A}(b_1)\Omega^{(//)}\right]^2\right). \tag{31}$$

We can write (31) in a simpler form. We pose $x_2 = h(x_1) = p_0 x_1$ (25) (*i.e.* $h_0 = 0$), $a_1 = 0$;

$$\begin{cases} f_{//}^{A}(x_1) = \dfrac{P}{\pi x_1}\,\overline{f}_{//}^{A}(x_1) \\ f_{\perp}^{A}(x_1) = \dfrac{P}{\pi x_1}\,\overline{f}_{\perp}^{A}(x_1) \end{cases} ; \tag{32}$$

$$G_0 = \frac{(1-\nu)P^2}{\pi^2 \mu l} ; \tag{33}$$

the normalized crack extension force $\tilde{G}(B) = G(B)/G_0$ then takes the form

$$\tilde{G}(B) = \left(\overline{f}_{\perp}^{A}(b_1)\Omega^{(\perp)}\right)^2 + \left(\overline{f}_{//}^{A}(b_1)\Omega^{(//)}\right)^2 \equiv \tilde{G}^{(\perp)}(B) + \tilde{G}^{(//)}(B) . \tag{34}$$

Next, a numerical analysis of our approximate solution (26) is performed.

IV - DISCUSSION

The crack-tip characteristic functions at $x_1 = b_1$ are known when the crack dislocation distributions D_J (26), equivalently the $\alpha_n^{(J)}$, have been estimated. This requires numerical resolution of (21). We use variables $\overline{t}_1 = \overline{x}_1 / \overline{ba_1}$ ($\overline{t}_1^{'} = \overline{x}_1^{'} / \overline{ba_1}$) under conditions $x_2 = h(x_1) = p_0 x_1$ and $a_1 = 0$. Using (26), we can write (21) as

$$\begin{cases} \dfrac{2\bar{f}^{A}_{//}(\bar{t}_1)}{1+\bar{t}_1} + \sum_{n=1}^{N}\left(\bar{f}^{A}_{\perp}(b_1)\tilde{D}^{C}_{\perp(n)}(\bar{t}_1)\alpha^{(\perp)}_n + \bar{f}^{A}_{//}(b_1)\left[\tilde{A}_{//(n)}(\bar{t}_1) - U_{n-1}(\bar{t}_1)\right]\alpha^{(//)}_n \right) = 0 \\ \dfrac{2\bar{f}^{A}_{\perp}(\bar{t}_1)}{1+\bar{t}_1} - \sum_{n=1}^{N}\left(\bar{f}^{A}_{\perp}(b_1)\left[-\tilde{A}_{\perp(n)}(\bar{t}_1) + U_{n-1}(\bar{t}_1)\right]\alpha^{(\perp)}_n + \bar{f}^{A}_{//}(b_1)\tilde{D}^{C}_{//(n)}(\bar{t}_1)\alpha^{(//)}_n \right) = 0 \end{cases} ; \quad (35)$$

$$\bar{f}^{A}_{//}(\bar{t}_1) = -\frac{(1-2\nu)\left(1+2(1+\nu)p_0^2\right)}{p_0^2}\ln\left(\frac{1+\bar{t}_1}{2}\right) - \frac{1-4\nu^2+p_0^2(1-2\nu^2)+p_0^4 2\nu(1+\nu)}{(1+p_0^2)^2},$$

$$\bar{f}^{A}_{\perp}(\bar{t}_1) = p_0\left(\frac{(1-2\nu)}{p_0^2}\ln\left(\frac{1+\bar{t}_1}{2}\right) + \frac{2\nu^2+2\nu-1}{1+p_0^2} + \frac{2\nu}{(1+p_0^2)^2}\right),$$

$$\bar{f}^{A}_{//}(b_1) = \bar{f}^{A}_{//}(\bar{t}_1 = 1),\ \bar{f}^{A}_{\perp}(b_1) = \bar{f}^{A}_{\perp}(\bar{t}_1 = 1); \quad (36)$$

$$\tilde{D}^{C}_{\perp(n)}(\bar{t}_1) = \frac{b_1}{2\pi}\int_{-1}^{1} d\bar{t}_1^{'}\ \frac{T_n(\bar{t}_1^{'})}{\sqrt{1-\bar{t}_1^{'2}}}\left(p_0(d_{//}-d_{\perp})+d_C\right),$$

$$\tilde{D}^{C}_{//(n)}(\bar{t}_1) = \frac{b_1}{2\pi}\int_{-1}^{1} d\bar{t}_1^{'}\ \frac{T_n(\bar{t}_1^{'})}{\sqrt{1-\bar{t}_1^{'2}}} d_C,$$

$$\tilde{A}_{//(n)}(\bar{t}_1) = \frac{b_1}{2\pi}\int_{-1}^{1} d\bar{t}_1^{'}\ \frac{T_n(\bar{t}_1^{'})}{\sqrt{1-\bar{t}_1^{'2}}} d_{//},$$

$$\tilde{A}_{\perp(n)}(\bar{t}_1) = \frac{b_1}{2\pi}\int_{-1}^{1} d\bar{t}_1^{'}\ \frac{T_n(\bar{t}_1^{'})}{\sqrt{1-\bar{t}_1^{'2}}} d_{\perp}; \quad (37)$$

U_{n-1} are the Chebychev polynomials of second kind. The convenient set of collocation $\bar{t}_1$ points is given by

$$\bar{t}_1 = \cos\frac{\bar{m}\pi}{N+1},\ \ \bar{m} = 1,\ 2\ ...N,\ (-1 < \bar{t}_1 < 1). \quad (38)$$

Using these values, (35) provides $2N$ linear algebraic equations in the unknown coefficients $\alpha^{(J)}_n$ which are easy to solve numerically. We use personal computer and MATLAB home license; therefore, the numerical results are qualitative. The precision depends on the step of integration $d\bar{t}_1^{'}$ in (37) and N; the smaller is $d\bar{t}_1^{'}$, the better is the convergency. Appropriate value for N is also wanted; it depends somewhat on $d\bar{t}_1^{'}$. We limit ourselves to $d\bar{t}_1^{'} = 10^{-5}$ with N= 30.

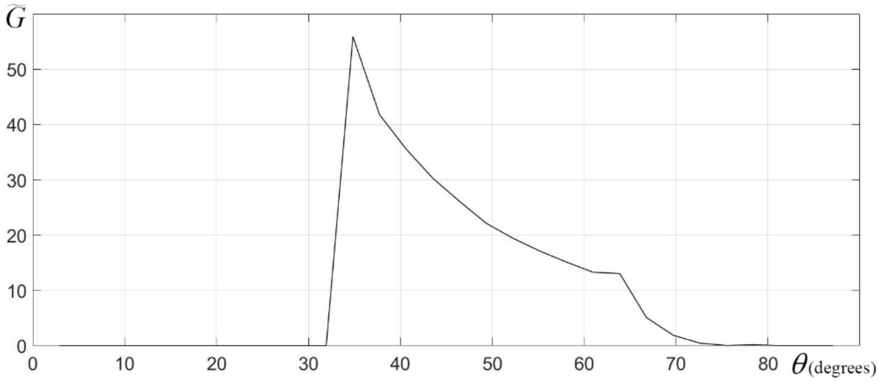

Figure 3 : *Normalized crack extension force $\tilde{G}$ (34) as a function of the crack inclination angle θ ; $\nu = 0.22\,; d\overline{t}_1^{'} = 2\;10^{-5}$*

In ***Figure 3*** is reported the reduced crack extension force $\tilde{G}$ (34) as a function of the inclination angle θ of the crack from the flat boundary (see ***Figure 1***). We take Poisson's ratio $\nu = 0.22$ for soda-lime glass. A net maximum ($\tilde{G}_M \approx 55$) for $\tilde{G}$ is seen at an angle $\theta_M \approx 33°$; θ_M doesn't change appreciably while $\tilde{G}_M$ decreases slowly with $d\overline{t}_1^{'}$ down to $d\overline{t}_1^{'} = 2\;10^{-5}$. Hence, the value for $\tilde{G}_M$ should be smaller. An experimentally observed value for θ is $\theta_E \approx 22°$ [1] (see also [2, 3]). The discrepancy with respect to θ_M is about 10°. A similar discrepancy between theory and experiment has been mentioned elsewhere [20]. Our expectation (see Section 1), that the crack system shown in ***Figure 1*** can evaluate the Hertzian cone crack, seems correct. An extremum for $\tilde{G}$ (34) with respect to θ is given by $\partial\tilde{G} / \partial\theta = 0$. This condition does not involve the shear modulus. Hence the crack angle is entirely controlled by the Poisson's ratio. The merit of the present modelling resides in its capability of providing an expression for the crack extension force *G*. Using the relation $G = 2\gamma$ at the maximum of *G*, we have a useful relation (in spherical indentation fracture too [1 - 3]) between applied load *P*, crack length *l* (see G_0 (33)) and crack inclination angle θ.

V - CONCLUSION

We have investigated fracture propagation in a three-dimensional elastic half-space subjected to the rectilinear contact pressure of a cylinder lying on the flat Ox_1x_3- plane boundary. The load is applied in the x_2- direction and over the Ox_3- contact line. Under such conditions, fracture over large distance occurs on a planar surface parallel to the cylinder x_3- axis and inclined by angle θ from x_1x_3 ***(Figure 1)***. The applied stress field $(\sigma)^A$ (2, 16) is the superposition $(\sigma)^a$ (15) of the stress fields due point loads distributed continuously along Ox_3 and induced normal stresses promoted by the Poisson's effect. This leads to the result that the x_2- component of the force $d\vec{F}_H$ (17) on any surface element of Ox_1x_3 is zero everywhere except on the contact line. Our method of stress analysis in the fractured medium consists in representing the crack by a continuous distribution of two straight edge dislocation families J (J= // and $\perp$) parallel to x_3 with Burgers vectors $\vec{b}_{//} = (b, 0, 0)$ and $\vec{b}_{\perp} = (0, b, 0)$ ***(Figure 1)***. The stress fields due to these dislocations J (18, 19) as well as those (20) of a straight screw dislocation parallel to x_3 with Burgers vector $\vec{b}_{III} = (0, 0, b)$ have been determined by a method involving Galerkin vectors (8, 10); these results are in complete agreement with those obtained in previous works [8, 9, 19] using different methods. The analysis of the crack under load leads to a system of two integral equations with Cauchy-type singular kernels implying the dislocation distribution functions D_J. The proposed solutions (26) are based on Erdogan and Gupta studies [14, 15]. Under such conditions, the relative displacement of the faces of the crack ϕ_J (27), crack-tip stresses $\bar{\sigma}_{ij}(s)$ (29) and crack extension force G (31, 34) per unit edge length, are calculated. The proposed expressions require a numerical analysis. Our qualitative numerical analysis (Section 4) reveals that G, expressed as a function of θ, exhibits a maximum at an angle $\theta_M \approx 33°$ with Poisson's ratio $\nu = 0.22$ for soda-lime glass; this is in reasonable agreement with the observed value $\theta_E \approx 22°$ in view of our approximative numerical analysis. Our expression for G (34) shows that the crack inclination angle θ is entirely controlled by the Poisson's ratio. This expression is equally helpful for indentation fracturing [1 - 3].

REFERENCES

[1] - F. C. ROESLER, *Proc. Phys. Soc. B*, 69 (1956) 981 - 1012
[2] - F. C. FRANK and B. R. LAWN, *Proc. R. Soc. Lond. A*, 299 (1967) 291 - 306
[3] - B. R. LAWN, "Fracture of Brittle Solids – Second Edition", Cambridge University Press, Cambridge, (1993)
[4] - P. N. B. ANONGBA, *Rev. Ivoir. Sci. Technol.*, 16 (2010) 11 - 50
[5] - P. N. B. ANONGBA, J. BONNEVILLE and A. JOULAIN, *Rev. Ivoir. Sci. Technol.*, 17 (2011) 37 - 53
[6] - P. N. B. ANONGBA, *Rev. Ivoir. Sci. Technol.*, 26 (2015) 76 - 90
[7] - P. N. B. ANONGBA, *Rev. Ivoir. Sci. Technol.*, 32 (2018) 10 - 47
[8] - A. K. HEAD, *Proc. Phys. Soc. London B*, 66 (1953) 793 - 801

[9] - T. MURA, In:" Advances in Materials Research", Ed. *Interscience Publications (H. Herman),* Vol. 3, (1968) 1 - 108
[10] - P. N. B. ANONGBA, *Rev. Ivoir. Sci. Technol.*, 26 (2015) 36 - 75
[11] - P. N. B. ANONGBA, *Rev. Ivoir. Sci. Technol.*, 28 (2016) 24 - 59
[12] - P. N. B. ANONGBA, *Rev. Ivoir. Sci. Technol.*, 30 (2017) 1 - 36
[13] - A. E. H. LOVE, "A treatise on the Mathematical Theory of Elasticity", Dover Publications, Inc., New York, 4^{th} ed., (1927)
[14] - F. ERDOGAN, *SIAM J. Appl. Math.,* 17 (1969) 1041 - 1059
[15] - F. ERDOGAN and G. D. GUPTA, *Quat. Appl. Math.*, 29 (1972) 525 - 534
[16] - P. N. B. ANONGBA, *Physica Stat. Sol. B,* 194 (1996) 443 - 452
[17] - P. N. B. ANONGBA and V. VITEK, *Int. J. Fract.*, 124 (2003) 1 - 15
[18] - B. A. BILBY and J. D. ESHELBY, In:" Fracture", Ed. *Academic Press (H. Liebowitz), New York,* Vol. 1, (1968) 99 - 182
[19] - A. K. HEAD, *Phil. Mag.*, 49 (1953) 92
[20] - M. M. CHAUDHRI, *Phil. Trans. R. Soc. A,* 373 (2015) 20140135